Available online at www.eccomasproceedia.org
Eccomas Proceedia COMPDYN (2023) 4125-4132

ECCOMAS
Proceedia

COMPDYN 2023
9th ECCOMAS Thematic Conference on
Computational Methods in Structural Dynamics and Earthquake Engineering
M. Papadrakakis, M. Fragiadakis (eds.)
Athens, Greece, 12-14 June 2023

MODELLING OF RIGID INCLUSIONS REINFORCED FOUNDATIONS TO INVESTIGATE THE FAILURE ENVELOPE IN THE V-M-H SPACE (COMPDYN 2023)

Ramon Alcala-Ochoa[*,1], **Zheng Li**[2], **Panagiotis Kotronis**[1] **and Giulio Sciarra**[1]

[1] Nantes Université, École Centrale Nantes, CNRS, Institut de Recherche en Génie Civil et Mécanique (GeM), UMR 6183, F-44000 Nantes, France.
e-mail: {ramon.alcala-ochoa,panagiotis.kotronis,giulio.sciarra}@ec-nantes.fr

[2] Laboratoire Centrifugeuses Géotechniques, Département GERS, Université Gustave Eiffel Campus de Nantes
Allée des Ponts et Chaussées, 44340 Bouguenais, France
e-mail: zheng.li@univ-eiffel.fr

Abstract. *The technique of ground reinforcement using Rigid Inclusions (RIs) is known to reduce settlements and enhance bearing capacity in soft soils. This approach leads to significant nonlinear interactions among the load transfer platform, piles, and the surrounding soil. The main objective of this paper is to identify the failure envelope of a shallow foundation on soft soil reinforced by RIs. This is a critical step in the safety assessment of this combined foundation system under static and dynamic (seismic) loading. The failure envelope, defined in the vertical force (V), bending moment (M) and horizontal force (H) space, is constructed using swipe tests from numerical simulations. A simple analytical formula is proposed to describe the failure envelope in V-M-H space. The failure envelope described by the proposed equation is the key ingredient for the macro-element modeling for the analysis of Soil-Structure Interaction of RIs foundation systems.*

Keywords: Shallow foundations, Reinforced soils, Ground improvement, Failure envelope

ISSN:2623-3347
Peer-review under responsibility of the organizing committee of COMPDYN 2023.
doi: 10.7712/120123.10706.20628

1 INTRODUCTION

As the demand for infrastructure grows, construction on soft ground becomes increasingly necessary. Consequently, it is crucial to design a reinforced foundation system with great care. Rigid Inclusions (RIs) are one of the soil improvement techniques for structures founded on compressible soils, as they can increase the soil-bearing capacity and limit the settlement of the superstructure. A RI reinforced foundation is composed of a shallow foundation, a compacted sand or gravel layer (Load Transfer Platform (LTP)) and vertical rigid inclusions. RI foundations are not only subject to vertical loads, but also to overturning moments and horizontal loads caused by wind or earthquake actions. Therefore, for an efficient design, understanding the coupling of vertical forces, V, bending moments, M, and horizontal forces, H, is mandatory. A failure envelope offers directly the bearing capacity that the foundation can provide. Multiple finite element method (FEM) simulations are carried out to investigate the complete failure locus of rigid inclusion reinforced foundations in the $V-M-H$ space. An analytical formula for the 3D failure surface is finally introduced.

2 NUMERICAL MODEL FOR A RI REINFORCED FOUNDATION

The numerical simulation is performed using the general purpose finite element code Cast3M [1]. The model is composed of a shallow foundation, a LTP, seven vertical rigid inclusions and a stiff soil layer based in the experimental model from a static centrifuge test conducted at the University Gustave Eiffel (Centrif−UGE) in the framework of the French national project − ASIRIplus-SDS [2]. The LTP layer is a mix of five Hostun sand fractions (HN38, HN34, HN31, HN04/08, HN06/1), according to [3] and is 1 m thick. The groundwater level is below the LTP at -1 m. A mixture of 80% Speswhite kaolin clay and 20% Fontainebleau sand serves as the compressible soil. This soft soil is 9.5 m thick, pre-consolidated at 120 kPa. The stiff soil bottom layer has a thickness of 4 m and is prepared with saturated dense Hostun (HN31) sand. The dimensions are given in the Figure 1.

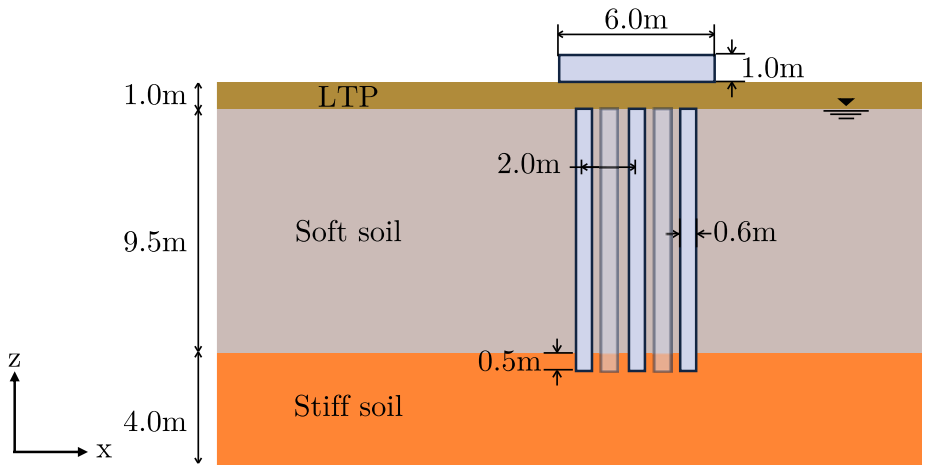

Figure 1: Centrifuge model of a circular shallow foundations with rigid inclusions (right): Geometry and soil stratigraphy, (prototype scale).

2.1 Calibration and validation of the soil characteristics

A linear elastic (EL) behavior is adopted for the footing and the RIs. To account for the sand nonlinearities in the LTP and stiff soil layers, a perfect elastoplastic Drucker-Prager (DP) constitutive model with a non-associated flow rule ($\psi \neq \varphi$) is considered. The DP parameters are closely matched to reproduce the classical Mohr–Coulomb model. The constitutive law is calibrated and validated using experimental triaxial tests from [3], with a relative density $I_{\mathrm{d}} = 0.9$, a friction angle $\varphi = 36°$ and a dilatancy angle $\psi = 2.5 - 4°$, see Figure 2 (a) and (b).

The compressible soil layer is numerically simulated using the critical state theory elastoplastic strain hardening Modified Cam-Clay model (MCC). The values of the normal consolidation, $\lambda = C_c/\ln(10)$, and swelling, $\kappa = C_s/\ln(10)$, slopes are determined from the compression, $C_c = 0.269$, and rebound, $C_s = 0.048$, indexes from the oedometer test S03 [4]. As shown in Figure 2 (c), a fair agreement of the numerical and experimental results is observed.

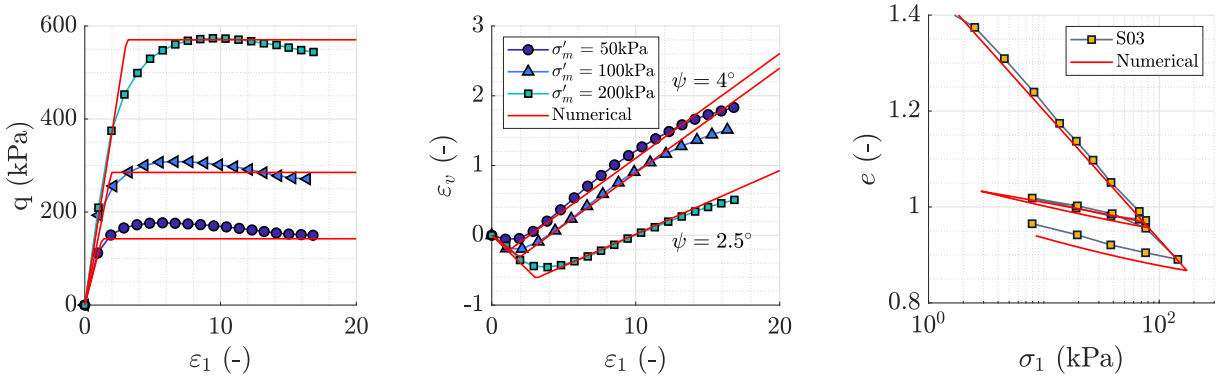

Figure 2: Experimental results (dots) and numerical calibration (red lines) (a) triaxial compression (b) triaxial extension test of Hostun mix sand, with a relative density $I_{\mathrm{d}} = 0.9$, from [3]; (c) experimental oedometric test results to stress vertical load increment, σ_a versus void ratio, e, from [4].

2.2 Finite element mesh and boundary conditions

The numerical simulation is performed using the general purpose finite element code Cast3M [1] respecting the dimensions of Figure 1. The dimensions of the mesh are 8B × 4B × 2.5B, (B= 6.0 m, the width of the foundation), and the number of elements is 148775. Due to symmetry, only half of the domain is considered. Preliminary analyses illustrated the areas of significant plastic strains, leading to a local mesh refinement at the vicinity of the piles and the footing edges, see Figure 3. Boundary conditions are applied by fixing the nodal displacements in the x, y and z directions at the base of the finite element model. The displacements at the other lateral boundaries are blocked in normal directions. No slippage is allowed between the soil and the RIs, because of the overconsolidation ratio $OCR > 1$, which leads to significant soil-pile confinement.

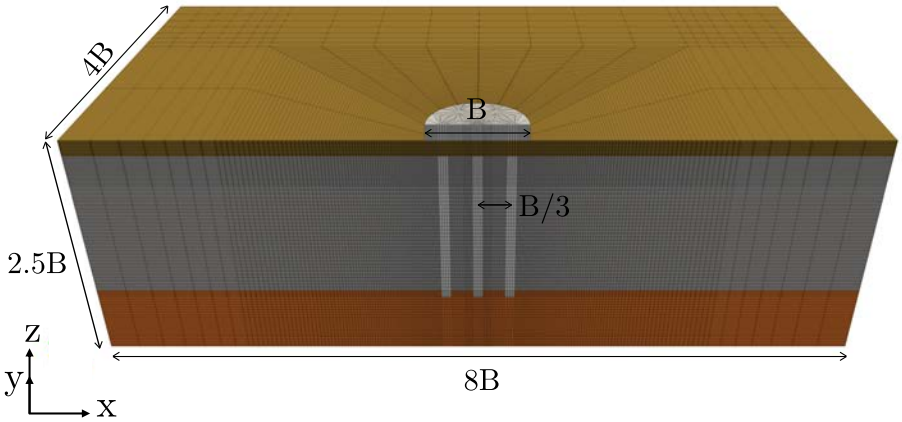

Figure 3: Finite element mesh and geometry for the foundation with RIs.

3 NUMERICAL STUDY OF THE 3D FAILURE ENVELOPE

3.1 Swipe tests

In order to determine the ultimate combined resistance of a shallow foundation reinforced by RIs, the displacement-controlled *swipe test* methodology is adopted. The fundamental idea comes from analogies with the hardening plasticity theory applied in critical state soil mechanics [5], in which the result is a load path that tracks along with the failure envelope (e.g., discussed in [6, 7, 8]). The sign conventions and the example of a load sweep in the $V - H$ space are shown in Figure 4. By assuming the maximum vertical displacement, w_0, and tracking the load paths generated by multiple combinations of horizontal displacements, u, and rotations, θ, the final 3D failure envelope can be numerically obtained.

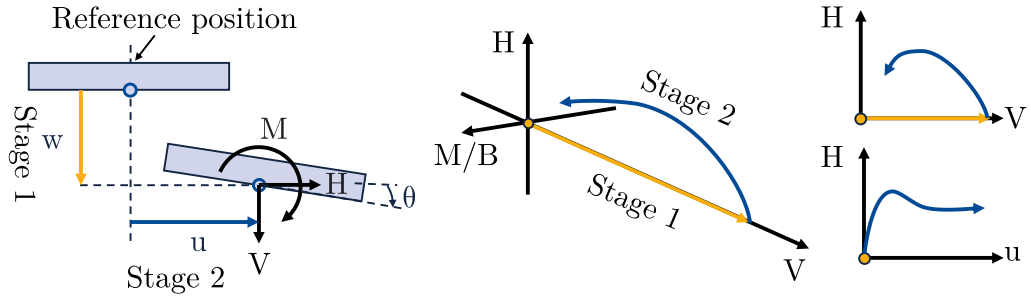

Figure 4: Swipe tests: stages, sign conventions, vertical and horizontal applied displacements, adapted from [9].

3.2 Vertical bearing capacity

First, a vertical displacement test is conducted to retrieve the vertical bearing capacity, V_0, and the corresponding vertical displacement, w_0. From the results shown in Figure 5 (a), the parameters can not be established, since the apparent failure is not observed. The tangent intersection method [10] is therefore adopted to approximate the maximal vertical bearing capacity, V_0 (red dot), calculated as the intersection of two tangents (black lines), the first corresponding to the initial slope and the second to the steeper portion of the final part of the curve. The final values are $V_0 = 4583$ kN and $w_0 = 0.09$ m.

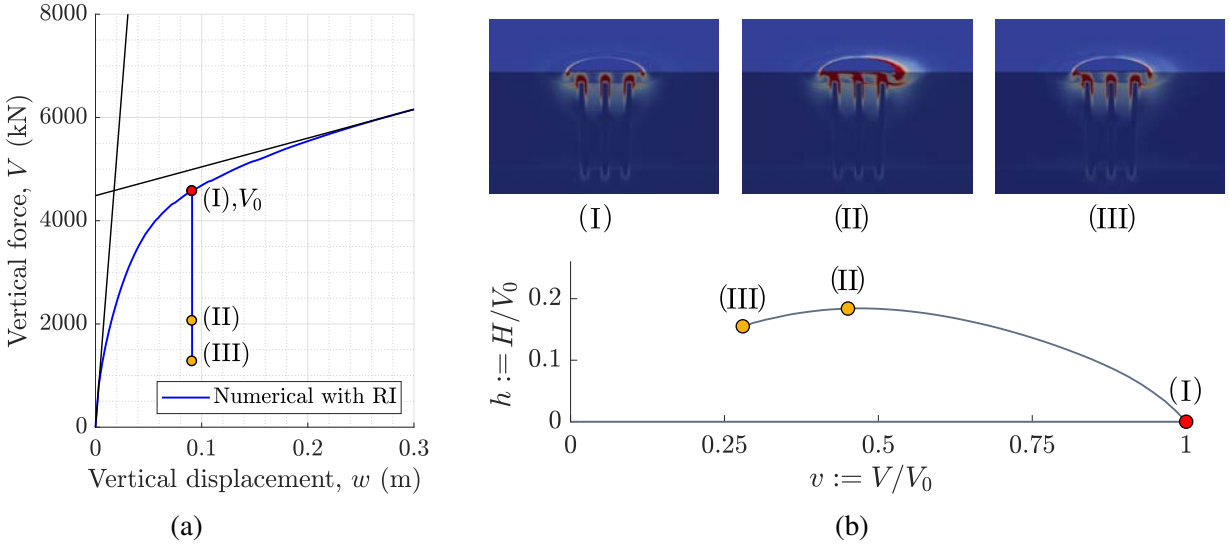

Figure 5: (a) Vertical displacement-load curve (blue line). Calculation of the maximal bearing capacity, V_0 (red dot), by the tangent intersection method (black lines) [10]. (b) Collapse mechanism in the normalized $v-h$ plane at (I) maximum vertical bearing capacity, (II) maximum horizontal normalized force and (III) end of the swipe test. The top part shows the plastic shear strain, γ^p, where the nonlinearities are concentrated in the red areas.

3.3 Numerical 3D failure envelope

The procedure described in subsection 3.1 is employed to find the full failure envelope. As mentioned, by assuming the maximum vertical displacement, w_0, the technique can generate a complete yield locus with only a few tests as the displacement combination tracks along with the failure envelope.

For an example of a purely horizontally driven swipe test, the evolution of the corresponding collapse mechanism can be visualized by plotting the plastic shear strain, γ^p, at specific load steps. This is illustrated in the top part of Figure 5 (b) for three steps zones in the normalized $v-h$ plane: (I) at maximum vertical bearing capacity, (II) at maximum horizontal normalized force and (III) at the end of the swipe test. From the figure is observed that the load is transferred to the piles through the LTP by the arching effect, and simultaneously, the vertical force applied to the RIs is transferred to the stiff soil layer. It can be drawn that the collapse mechanism is mainly developed in the LTP layer.

The numerical 3D failure envelope, resulting from sixty-two numerical swipe tests, is shown (in grey) in the $v-h-m$ normalized space in Figure 6 (a). The representation of a cut in the $m-h$ plane is shown in yellow for $v = 0.5$.

4 ANALYTICAL 3D FAILURE ENVELOPE OF RI REINFORCED FOUNDATIONS

This section aims to approximate the failure envelope of subsection 3.3, found using numerically reproduced swipe tests, with an appropriate closed-form mathematical formulation. It can be concluded from Figure 6 (a) that:

- $h-m$ plane: results have the form of an inclined ellipse centred at the origin.
- $v-h$ plane: the failure envelope has a parabolic form. Starting from V_0, its size increases with the decreasing of vertical force v. In this plane, the maximum is reached at a critical

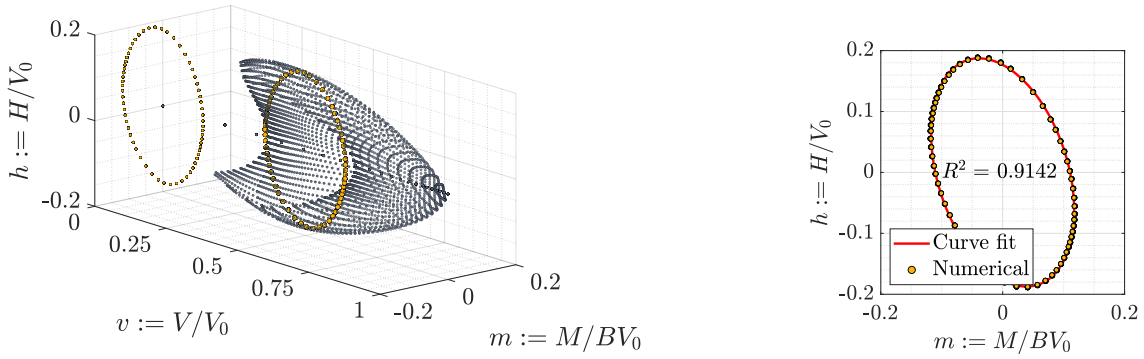

(a) (b)

Figure 6: (a) Failure envelope obtained from sixty-two numerical swipe tests. The representation of a cut in the $m - h$ plane is shown in yellow for $v = 0.5$ (b) Curve fitting of the numerical data using the direct least square fitting of ellipses [11].

point close to $v = 0.45 - 0.5$ (also observed in Figure 5 (b)). A decreasing trend is observed afterwards for lower values of v.

The main idea to find the analytical formula is i) to calibrate the three parameters (a, b, c) of the inclined ellipse general equation $ay^2 + bz^2 + cyz - a^2b^2 = 0$ with the numerical results corresponding to the critical point of the vertical forces, taken hereafter equal to $v = 0.5$; and then ii) to use the parabola of the form $4x(1 - x) = 0$ (that has a peak value equal to 1 at 0.5 and being 0 at 0 and 1) to automatically control the different ellipses' size.

The 'cigar shape' parabolic ellipsoid envelope, used in the literature for shallow foundations on sand, see [7, 12, 13, 14], among others, is therefore again adopted hereafter. The complete expression, in terms of normalized loads, can be expressed as:

$$f(v, m, h) = \frac{m^2}{m_0^2} + \frac{h^2}{h_0^2} - 2a_0\frac{mh}{m_0 h_0} - [4v(1 - v)]^2 = 0 \tag{1}$$

where m_0 and h_0 determine the failure envelope shape and size and represent the intersection of each ellipse in the normalized $v - m$ and $v - h$ planes, respectively. a represents the cross-section tilt angle in the $m - h$ plane, measured from the h axis.

In order to calibrate the ellipse, the direct method for least square fitting of ellipses is employed [11], see Figure 6 (b). The three parameters are found to be

$$h_0 = 0.1766 \quad m_0 = 0.1105 \quad a_0 = -0.3325 \tag{2}$$

The final parabolic ellipsoid representation of Equation 1 is shown in yellow, together with the numerical swipe test results as grey dots, in Figure 7. A high correlation is obtained ($R^2 = 0.9142$), evidencing that the suggested formula is suitable for design purposes and the development of simplified modelling strategies, such as novel macro-elements.

5 CONCLUSIONS

This paper presents a 3D finite element model to numerically reproduce the ultimate combined resistance of RIs foundations using swipe tests. The analytical formula defined by Equation 1 and Equation 2 is proposed for the failure envelope of a rigid inclusion reinforced foundation

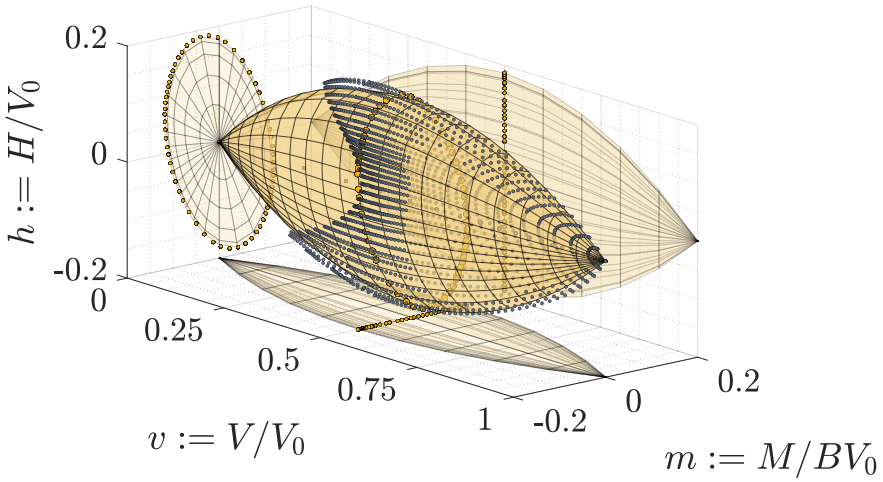

Figure 7: Normalized failure envelope in $v-m-h$ space. Proposed analytical formula (yellow) and numerical swipe test results (gray dots).

on soft soil. Practitioners can use the proposed analytical equation of the failure envelope to quantify the bearing capacity under complex 3D loading and researchers to develop novel macroelements. More details on this work can be found in [15].

REFERENCES

[1] CEA, "Cast3m," 2001. http://www-cast3m.cea.fr/.

[2] ANR, "Soil improvement by rigid inclusions: Seismic and dynamic loading – ASIRIplus-SDS," 2020.

[3] G. Baudouin, *Sols renforcés par inclusions rigides : modélisation physique en centrifugeuse de remblais et de dallage*. PhD thesis, Université de Nantes. Faculté des sciences et des techniques, 2010. 2010NANT2046.

[4] S. Escoffier, Z. Li, and C. Soriano, "Data Report no. 2 ASIRI+ Project amélioration des sols par inclusions rigides: sollicitations dynamiques et sismiques," tech. rep., Université Gustave Eiffel, 9 2022.

[5] A. Schofield and P. Wroth, "Critical state soil mechanics," *McGraw Hill, London*, 1968.

[6] F. Tan, *Centrifuge and theoretical modelling of conical footings on sand*. PhD thesis, University of Cambridge, Cambridge, UK, 1990.

[7] G. Gottardi and R. Butterfield, "On the bearing capacity of surface footings on sand under general planar loads," *Japanese Society of Soil Mechanics and Foundation Engineering*, vol. 33, pp. 68–79, 9 1993.

[8] S. Grange, *Modélisation simplifiée 3D de l'interaction sol-structure: application au génie parasismique.* PhD thesis, Institut National Polytechnique de Grenoble - INPG, June 2008.

[9] R. Butterfield, G. T. Houlsby, and G. Gottardi, "Standardized sign conventions and notation for generally loaded foundations," *Geotechnique*, vol. 47, pp. 1051–1054, 1997.

[10] A. Hirany and F. H. Kulhawy, "Conduct and interpretation of load tests on drilled shaft foundations: Volume 1, detailed guidelines: Final report," tech. rep., Cornell University, 7 1988.

[11] A. Fitzgibbon, M. Pilu, and R. B. Fisher, "Direct least square fitting of ellipses," *IEEE Trans. Pattern Analysis and Machine Intelligence*, vol. 21, pp. 987–996, 5 1999.

[12] R. Nova and L. Montrasio, "Settlements of shallow foundations on sand," *Géothecnique*, vol. 41, pp. 243–256, 1991.

[13] M. J. Cassidy, *Non-linear analysis of jack-up structures subjected to random waves*. PhD thesis, University of Oxford, 1999.

[14] G. Gottardi, G. T. Houlsby, and R. Butterfield, "Plastic response of circular footings on sand under general planar loading," 6 1999.

[15] R. Alcala-Ochoa, Z. Li, P. Kotronis, and G. Sciarra, "3D failure envelope of RI foundations," 2023. Unpublished, to be submitted to Géotechnique.